Available online at www.sciencedirect.com
SCIENCE DIRECT
Geochimica et Cosmochimica Acta 70 (2006) 1807–1820
Geochimica
www.elsevier.com/locate/gca

LA-MC-ICPMS Pb–Pb dating of rutile from slowly cooled granulites: Confirmation of the high closure temperature for Pb diffusion in rutile

Julie K. Vry [a,*], Joel A. Baker [a,b]

[a] School of Earth Sciences, Victoria University of Wellington, P.O. Box 600, Wellington, New Zealand
[b] Danish Lithosphere Centre, Øster Voldgade 10, DK-1350 Copenhagen K, Denmark

Received 12 August 2005; accepted in revised form 8 December 2005

Abstract

Rapid Pb–Pb dating of natural rutile crystals by laser ablation multiple-collector inductively coupled plasma mass spectrometry (LA-MC-ICPMS) is investigated as a tool for constraining geological temperature–time histories. LA-MC-ICPMS was used to analyse Pb isotopes in rutile from granulite-facies rocks from the Reynolds Range, Northern Territory, Australia. The resultant ages were compared with previous U–Pb zircon and monazite age determinations and new mica (muscovite, phlogopite, and biotite) Rb–Sr ages from the same metamorphic terrane. Rutile crystals ranging in size from 3.5 to 0.05 mm with $\leqslant$20 ppm Pb were ablated with a 300–25 μm diameter laser beam. Crystals larger than 0.5 mm yielded sufficiently precise $^{206}Pb/^{204}Pb$ and $^{207}Pb/^{204}Pb$ ratios to correct for the presence of common Pb, and individual rutile crystals often exhibited sufficient Pb isotopic heterogeneity to allow isochron calculations to be performed on replicate analyses of a single crystal. The mean of 12 isochron ages is 1544 ± 8 Ma (2 SD), with isochron ages for single crystals having uncertainties as low as ±1.3 Myr (2 SD). The ^{207}Pb–^{206}Pb ages calculated without correction for common Pb are typically <0.5% higher than the common-Pb-corrected isochron ages reflecting the very minor amounts of common Pb present in the rutile. The LA-MC-ICPMS method described samples only the outer 0.1–0.2 mm of the rutile crystals, resulting in a grain size-independent apparent closure temperature (T_c) for Pb diffusion in rutile that is less than the T_c of monazite $\leqslant$0.1 mm in diameter, but significantly higher than the Rb–Sr system in muscovite (550 °C), phlogopite (435 °C) and biotite (400 °C). Even small rutile crystals are extremely resistant to isotopic resetting. For the established slow cooling rate of ca. 3 °C/Myr, the T_c for Pb diffusion in the analysed rutile is ca. 630 °C. This is in excellent agreement with recent experimental results that indicate that rutile has a higher T_c than previously thought (ca. 600–640 °C for rutile 0.1–0.2 mm diameter cooled at 3 °C/Myr; near 600 °C [Cherniak D.J., 2000. Pb diffusion in rutile. *Contrib. Mineral. Petrol.* **139**, 198-207], versus 400 °C [Mezger, K., Hanson G.N., Bohlen S.R., 1989a. High precision U–Pb ages of metamorphic rutile: applications to the cooling history of high-grade terranes. *Earth Planet. Sci. Lett.* **96**, 106–118.] for 1 °C/Myr), and with current T_c estimates for monazite and other high temperature geochronometers, which have been revised upwards in recent years. The new rutile ages, together with the other geochronological data from the region, support the interpretation that the Reynolds Range underwent prolonged slow cooling on a conductive geotherm, under nearly steady-state conditions. Slow cooling at ca. 3 °C/Myr persisted for at least 40 Myr followed the peak of high-*T*/low-*P* metamorphism to granulite-facies conditions, and probably continued at ca. 2–3 °C/Myr for ca. 200 Myr overall.

1. Introduction

Rutile is the most common and stable polymorph of TiO_2. It occurs widely as an accessory mineral, and it has been shown to yield precise U–Pb ages. Rutile has been used for nearly two decades as a relatively low-temperature geochronometer that can provide timing constraints on metamorphic cooling (e.g., Mezger et al., 1989a,b, 1991; Heaman and Parrish, 1991; Miller et al., 1996; Santos Zalduegui et al., 1996; Davis, 1997; Di Vincenzo et al., 1997; Indares and Dunning, 2001; Treloar et al., 2003;

* Corresponding author. Fax: +64 4 463 5186.
E-mail address: julie.vry@vuw.ac.nz (J.K. Vry).

0016-7037/$ - see front matter © 2005 Elsevier Inc. All rights reserved.
doi:10.1016/j.gca.2005.12.006

Timmermann et al., 2004). However, recent experimental results (Cherniak, 2000) place this historical use of rutile as low-temperature geochronometer in question. The suggestion that rutile has amongst the lowest closure temperatures (T_c) for Pb diffusion in common accessory minerals (ca. 400 °C) was based on an empirical calibration of the T_c of Pb in rutile against temperature–time histories for two North American metamorphic terranes that are constrained by other chronometers (Mezger et al., 1989a). In contrast, the experimental results indicate that the T_c for Pb diffusion in rutile is considerably higher than previously thought and, furthermore, that rutile has a high activation energy for Pb diffusion and so should be resistant to later isotopic resetting (Cherniak, 2000). The experimental results thus favour an interpretation that the Pb–Pb system in rutile should serve as a robust high-temperature geochronometer that could provide an alternative to monazite or titanite dating, depending upon grain size. If correct, this conclusion is important because rutile, unlike other lower temperature (400–550 °C) chronometers such as the Rb–Sr system in micas, could escape isotopic resetting in polymetamorphic terranes, yielding valuable additional or corroborative geochronological information about high-temperature metamorphism and the cooling that follows it.

However, experimental calibrations of closure temperatures in minerals are not without problems when applied to natural examples. Experiments are often carried out at temperatures much higher than those in the natural systems, though those of Cherniak (2000) were carried out at temperatures down to and below the metamorphic crystallization temperatures for our samples from the Reynolds Range. Also, experiments are not normally conducted in the presence of other minerals that may act as a sink for the daughter isotope of the decay system of interest. For example, Jenkin (1997) and Jenkin et al. (2001) have shown that the presence or absence of a Sr-sink in a rock plays a critical role in the effective T_c for the Rb–Sr system in biotite. In order to help resolve the current uncertainty as to the T_c of Pb in natural rutile, we have carried out a new empirical determination of the T_c using natural rutile from a site for which the timing of granulite-facies metamorphism (ca. 1584 Ma), the high-temperature metamorphic pressure-temperature (P–T) history, and the subsequent slow cooling (3 °C/Myr) are all well-constrained (Vry and Cartwright, 1994; Vry et al., 1996; Williams et al., 1996; Buick et al., 1998; Buick et al., 1999; Rubatto et al., 2001). Even though a lower-temperature metamorphic event did affect the area much later during the 400–300 Ma Alice Springs orogeny (Teyssier, 1985; Shaw et al., 1991, 1992), the initial cooling that followed the metamorphism to high-T and low-P granulite-facies conditions was slow and prolonged, with melt crystallization continuing over ca. 30 Myr (Williams et al., 1996; Buick et al., 1999; Rubatto et al., 2001). This slow cooling at high temperatures should be ideal for a calibration of T_c as it ensures that the uncertainties in the age determinations are small with respect to the whole duration of the cooling episode, thus allowing for a better estimation and comparison of closure temperatures.

In this paper, we present the first Pb–Pb ages for rutile obtained using laser ablation multiple-collector inductively coupled plasma mass spectrometry (LA-MC-ICPMS). An ultraviolet laser ablation system coupled to an MC-ICPMS has been used to measure Pb isotope ratios of natural rutile crystals from the Reynolds Range. This method rapidly provides a wealth of data, but still yields analytical uncertainties <0.5% on the calculated Pb–Pb ages for these rutile crystals, more than adequate for constraining temperature–time paths in slowly cooled metamorphic terranes that are Proterozoic or older in age. The rutile age results are then integrated with other geochronological data including: (1) previously published results of SHRIMP II dating of monazite and zircon from the same sample site and, in some cases, from the same samples (Vry et al., 1996) as well as from other nearby parts of the Reynolds Range, and (2) new Rb–Sr ages on muscovite, phlogopite, and biotite from the Reynolds Range localities. These new data (1) support recent experimental results by Cherniak (2000) that indicate that rutile is a high temperature geochronometer; (2) better constrain the closure behaviour of Pb diffusion in rutile relative to zircon and monazite; and (3) improve understanding of the cooling history of this classic example of a high-T/low-P metamorphic terrane.

2. Geological setting

The Reynolds Range is a 130-km-long, northwest-trending range of hills located ca. 120 km to the NNW of Alice Springs, Northern Territory (Fig. 1), in the Arunta Inlier, a Proterozoic complex of metamorphic and igneous rocks in central Australia. The study area is composed largely of metasedimentary rocks that have undergone a protracted history of repeated deformation, granitic magmatism, and contact and regional metamorphism at shallow crustal levels (<15 km depth). The metamorphic grade increases along the structural–stratigraphic strike of the range from greenschist-facies in the northwest, to high-temperature and low-pressure (high-T, low-P; 750–800 °C and ca. 4–5 kbar) granulite-facies in the southeast. Most, but not all, of the features in the southeast Reynolds Range reflect conditions during the final high-grade regional metamorphism and deformation episode. This is currently interpreted to have been a single, remarkably long-lived (ca. 1594–1555 Ma) event, with melt crystallization and local fluid flow continuing for ca. 30 Myr over the period 1587–1557 Ma during very slow cooling at ca. 3 °C/Myr, in a stable high geothermal regime (Vry and Cartwright, 1994; Williams et al., 1996; Buick et al., 1998; Buick et al., 1999; Rubatto et al., 2001). As discussed later in this paper, the results of the present study support this interpretation and suggest that despite the shallow crustal setting slow cooling at 2–3 °C/Myr and could have prevailed for up to 200 Myr.

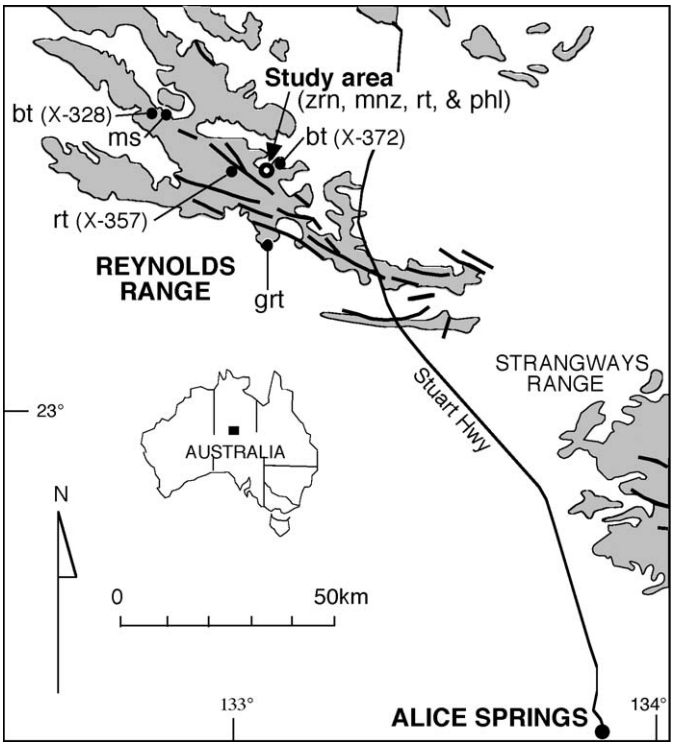

Fig. 1. Simplified map of the Reynolds Range, Northern Territory, Australia, showing localities for the samples that form the basis of this study (ms, muscovite; rt, rutile; zrn, zircon; mnz, monazite; phl, phlogopite; bt, biotite; and grt, garnet).

The rutile occurs in unusual coarse-grained Mg- and Al-rich rocks that have already proven specifically useful for constraining the high-temperature regional metamorphic *P–T* and timing history of the region. These granulite-facies rocks crop out in large pods, a few tens of metres wide by several tens of metres long, along a stratigraphic boundary in the SE Reynolds Range. The surrounding Early Proterozoic Lander Rock beds are high grade quartz-rich and pelitic metasedimentary rocks that were deposited through to ca. 1838 Ma. Four of the five rutile-bearing samples were collected within a few 10 or 100 s of metres of each other, from sites in and along the margins of a large pod of near Sandy Creek (Vry and Cartwright, 1994, 1998; Vry et al., 1996; Fig. 1). The remaining rutile-bearing sample (X-357) was collected approximately 6 km to the west of the others, from a related rock type.

The region has a polymetamorphic history that includes an early episode of regional metamorphism, followed later by contact metamorphism and associated metamorphic fluid/rock interaction related to the emplacement of granites at ca. 1820–1800 Ma. Diagenetic-hydrothermal alteration zones containing abundant Mg-rich chlorite formed locally as the early granites cooled, and the unusual Mg- and Al-rich rocks in the pods formed by granulite-facies metamorphism of these alteration zones at ca. 1584 Ma, during the final (ca. 1594–1555 Ma) high grade metamorphic episode (Williams et al., 1996; Vry and Cartwright, 1998; Rubatto et al., 2001). Because the rocks in the pods crystallized from unusual new precursor materials that formed after the early regional and contact metamorphic history had already taken place, the rutile-bearing samples studied here record an isolated part of the complex overall metamorphic history.

The study site was selected for the following reasons:

(1) Many of the rocks contain abundant, relatively large (ca. 2–4 mm) rutile as part of the peak metamorphic assemblage. Large rutile crystals without any visible overgrowths were initially sought to best constrain their oldest cooling age, which should be associated with the highest T_c for Pb diffusion for rutile from the study area, and by inference, other terranes with similar slow cooling rates. Textural evidence clearly demonstrates that the rutile studied here is part of the peak metamorphic assemblage and not of a detrital or secondary hydrothermal origin. Coarse rutile occurs as a characteristic mineral only in the pods of high-grade Mg- and Al-rich rocks, not in the country rocks. The coarse rutile crystals are texturally well-equilibrated with the other high-grade metamorphic minerals in the pods, such as spinel, orthopyroxene, gedrite, clinohumite, kornerupine, and cordierite, and near the margins of the pods, the coarse rutile can be intergrown with prismatic sillimanite. The coarse rutile never occurs in textural association with any minerals formed by lower temperature retrograde alteration of the high grade assemblages, and it does not typically occur as mineral inclusions in other high grade minerals.

(2) The timing of high-temperature regional metamorphism in the Reynolds Range is well known, based on results of detailed U–Pb SHRIMP age determinations of zircon and monazite from rocks collected at this exact sample site and from the wider region as a whole (cf. Vry et al., 1996; Williams et al., 1996; Rubatto et al., 2001; Figs. 2, 3). Metamorphic monazite (ca. 1584 Ma in the immediate vicinity of the study site) is abundant in amphibolite- and granulite-facies rocks in the Reynolds Range, whereas most of the zircon is inherited (Vry et al., 1996; Rubatto et al., 2001). New overgrowths of metamorphic zircon are only recorded in granulite-facies rocks where melt was present ($\geqslant$700 °C), and in the rocks from the Mg- and Al-rich pods, where the metamorphic zircon and monazite ages are comparable (Vry et al., 1996; Rubatto et al., 2001). The geological evidence, described above, makes it unlikely that age data from the coarse rutile studied here would be complicated by geochronological inheritance, and the availability of SHRIMP zircon and monazite data provides a rare opportunity to directly compare the isotopic closure behaviour of rutile, monazite and zircon in samples where inheritance in the zircon and monazite has already been specifically addressed. No evidence of inheritance has been found in any monazite from the pods of Mg- and Al-rich rocks,

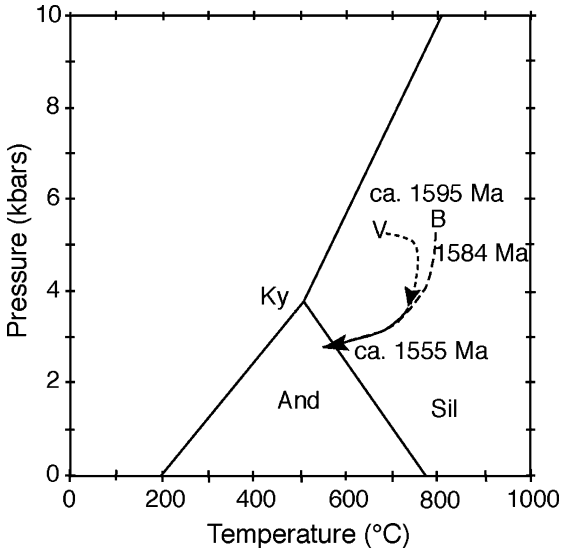

Fig. 2. Metamorphic P–T path for granulite-facies metamorphism in Reynolds Range (after V—Vry and Cartwright, 1994; for rutile sample location and B—Buick et al., 1998). Age constraints for the P–T path are based on U–Pb SHRIMP dating of zircon overgrowths (1596 ± 4–1562 ± 4 Ma; $T \geqslant 700$ °C) and monazite (1594 ± 5–1555 ± 6 Ma; $T \geqslant 650$–700 °C; cf. Vry et al., 1996; Williams et al., 1996; Rubatto et al., 2001).

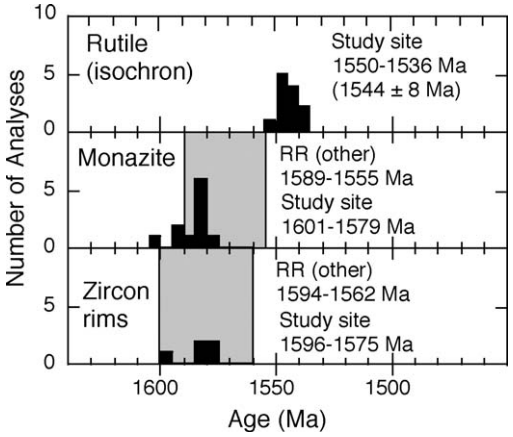

Fig. 3. Comparison of results of $^{207}Pb/^{206}Pb$ radiogenic age determinations for zircon rims and monazite (Vry et al., 1996; Williams et al., 1996; Rubatto et al., 2001), and the Pb–Pb ages obtained on rutile in this study. The plotted rutile ages are the Pb–Pb isochrons calculated with a common Pb point. The grey boxes for the zircon and monazite ages encompasses all the available dates on these minerals from high-grade parts of the Reynolds Range (RR), whereas the solid black histograms only compile data from the same locality as the dated rutiles.

though this is not the case everywhere throughout the high grade parts of the Reynolds Range (see Vry et al., 1996; Rubatto et al., 2001).

(3) The metamorphic P–T–t path, from just prior to and during the peak of granulite-facies metamorphism, through to the subsequent early retrogression at high temperatures (Fig. 2), has been carefully defined for this sample collection site (Vry and Cartwright, 1994) and subsequently confirmed for other high-grade parts of the Reynolds Range (Buick et al., 1998). The overall cooling rate for the early retrogression at high temperatures is well-defined and slow (ca. 3 °C/Myr for ca. 26–30 Myr; Williams et al., 1996; Buick et al., 1998; Rubatto et al., 2001). This extended period of cooling should enable precise determination of the T_c for Pb diffusion in rutile.

(4) The Mg- and Al-rich rocks also contain abundant phlogopite–biotite. This is amenable to Rb–Sr dating that could potentially better constrain the lower temperature cooling history of the Reynolds Range.

3. Samples

In this study, we present new Pb–Pb age data for rutile from five samples, Rb–Sr age data for phlogopite and biotite from the same and nearby sample sites, and a Rb–Sr muscovite age from amphibolite-facies rocks located nearby. The following section briefly describes the petrographic characteristics of each sample and previous geochronological data obtained on each sample, where available.

3.1. Rutile samples

KRN-6: Sample KRN-6 was selected for detailed study because it contains abundant rutile, including the largest rutile crystals (up to 4 mm) found in any of the Reynolds Range samples. Pb–Pb SHIRMP age determinations for zircon also exist for this sample, and monazite results are available from the immediate sample site, allowing the timing of closure for Pb diffusion in zircon, monazite and rutile to be directly compared. The overgrowths on zircon in this sample have $^{207}Pb/^{206}Pb$ ages of 1575.0 ± 5.4 to 1596.0 ± 3.8 Ma, (1 SD, $n = 4$; Figs. 2 and 3). Sample KRN-6 consists largely of coarse-grained (to ca. 6 cm) radiating crystals of pale grey kornerupine and abundant, coarse, randomly oriented blades of pale brown gedrite, with minor rutile and phlogopite, and abundant accessory ilmenite, zircon and, locally, tourmaline. In places, corroded relics of orthopyroxene texturally predate the growth of gedrite and, elsewhere, intergrowths of orthopyroxene and cordierite may texturally predate kornerupine growth. Phlogopite from this rock was also Rb–Sr dated.

X-16: Sample X-16 is a coarse-grained rock consisting of randomly oriented orthopyroxene, a bright orange humite-group mineral, green spinel with magnetite exsolution, minor rutile, phlogopite, and ilmenite, and accessory zircon, wagnerite and apatite. Gedrite is similar in size to the orthopyroxene, but texturally post-dates it. The rutile grains from this sample were ca. 0.65–0.85 mm in diameter.

X-195 and X-200: Sample X-195 consists of a coarse, symplectitic intergrowth of randomly oriented cordierite and orthopyroxene, with radiating blades of gedrite (all ca. 5–10 mm long). The rock also contains abundant crystals of rutile (0.01–0.20 mm), and accessory phlogopite ($\leqslant$1 mm) and ilmenite. The mafic minerals can exhibit a

minor, narrow alteration zone of fine-grained sub-calcic amphibole along grain boundaries and fractures. The analysed rutile crystals were typically $\leqslant$0.1 mm in diameter. Sample X-200 is similar to X-195, but slightly coarser grained, and poorer in phlogopite, which occurs in the central parts of the large orthopyroxene crystals. The rock also contains accessory zircon. The analysed rutile crystals from X-200 were ca. 0.1 mm in size.

X-357: The rock consists mainly of large subhedral blocky crystals of cordierite (up to 5 mm) that may contain small rounded tourmaline crystals, as well as rutile, zircon and/or monazite and, in some areas, abundant fine prismatic sillimanite that is randomly oriented. Locally, tourmaline containing abundant fine sillimanite forms infillings between cordierite crystals. The rutile crystals (up to 0.5 mm; analysed crystals were typically ca. 0.2 mm in size) can be intergrown with the coarse prismatic sillimanite that occurs abundantly, together with very minor quartz, in bands that cut across cordierite and fine prismatic sillimanite.

3.2. Mica samples

X-14 (phlogopite): This rock is from the same specific study area as the rutile samples. The sample consists mainly of coarse green phlogopite, with minor coarse green spinel that is locally rimmed by sapphirine. The phlogopite appears pristine and the spinel is nearly so, with only a few rare traces of later alteration to a fine-grained mixture of corundum + magnetite ± chlorite along fractures and grain margins.

V91-4 (phlogopite): This rock was collected at the margin of the same pod as the rutile samples, and is interpreted to be related in its origins to the formation of the pods. The rock is texturally pristine, consisting of cordierite, quartz, and green phlogopite (all to ca.1 mm), with scattered large (to 3 cm) rounded orthopyroxene poikiloblasts. The mineral assemblage is interpreted to have formed at high temperatures near the peak of the granulite facies regional metamorphism, as the associated deformation waned (Vry and Cartwright, 1994).

X-23 (phlogopite): This rock is like X-14 and was collected less than 2 m away from it. The phlogopite is dark greenish-black in hand sample, and appears to be entirely pristine under the microscope, but the associated spinel has been completely replaced by a fine-grained mixture of corundum + magnetite ± chlorite.

X-328 (biotite): X-328 is a medium-grained quartz schist that shows evidence of both early contact metamorphism, which produced andalusite porphyroblasts up to 1 cm long, and later regional metamorphism in the biotite stability field at temperatures above 550 °C (Rubatto et al., 2001). The growth of small random biotite crystals predated the growth of andalusite during the early contact metamorphism. During the later regional metamorphism, which reached granulite-facies conditions in areas further to the SE, the biotite outside those porphyroblasts coarsened and was realigned, forming a foliation. This coarse biotite was analysed in the present study; it appears unaltered under the microscope.

X-372 (biotite): This rock is a sample of the Yaningidjara Orthogneiss—a coarse-grained, multiply deformed, K-feldspar megacrystic granite with biotite, quartz, plagioclase, and accessory zircon and monazite. This granite was emplaced into the Lander Rock beds in the southeast Reynolds Range, where it produced a distinct contact aureole. The large (to 8 cm) andalusite porphyroblasts that formed in the aureole were replaced by sillimanite and other higher-T mineral assemblages during the later high-grade metamorphism. SHRIMP Pb–Pb ages for zircon from this sample (1806 ± 6 Ma) appear to record magmatic crystallization, whereas monazite records a late stage of the high-grade metamorphism (1566 ± 2 Ma) (Vry et al., 1996; Williams et al., 1996; Buick et al., 1998; Buick et al., 1999; Rubatto et al., 2001).

X-324 (muscovite): This sample was collected from the sheared margin of the Mt. Airy Orthogneiss, a ca. 1800–1820 Ma K-feldspar megacrystic granitoid. The clean coarse-grained muscovite analysed in the present study is part of the original mineral assemblage of the granite, which also includes quartz, K-feldspar, plagioclase, biotite, and accessory apatite. The shearing produced spaced zones of grain size reduction associated with abundant extremely fine-grained white mica. The later low-*P* regional metamorphism reached conditions near 600 °C, not far below the stability of sillimanite, in this region (Rubatto et al., 2001), and following that event both this and the higher grade region to the SE would have cooled together.

4. Analytical methods

4.1. Sample materials and preparation

Rutile: Rutile-bearing rock samples were lightly crushed in a steel percussion mortar and sieved. Rutile crystals or rock fragments containing visible rutile were hand-picked under a binocular microscope from the sieved splits or from magnetically separated sieve splits. The larger rutile crystals or fragments of rock containing smaller rutile crystals were mounted on glass slides with epoxy resin. The rutile was not subjected to any grinding or polishing prior to LA-MC-ICPMS analysis.

Mica: The mica samples were separated into different aliquots by repeatedly lightly crushing in an agate mortar, and then sieving the material through a 200-μm plastic screen. This process progressively produced sequentially purer aliquots of mica from each sample as low Rb/Sr inclusions such as apatite are removed from the mica leaves and pass through the sieve. In most cases, two different aliquots of mica prepared in this way were analysed for Rb–Sr isotopes.

4.2. Rb–Sr isotopic analysis

Mica separates for Rb–Sr analyses were weighed (ca. 0.05 g) and dissolved in $HF–HNO_3$ on a hotplate at

140 °C. After complete dissolution, the mica solution was quantitatively split into two fractions and one fraction spiked with a mixed ^{87}Rb–^{84}Sr isotopic tracer for Rb–Sr concentration determinations. This procedure circumvents the complexity of accounting for the presence of spike when undertaking Rb interference corrections during the Sr isotope measurement during MC-ICPMS analysis (Waight et al., 2002a,b). Rubidium and Sr were separated with 2 M HCl on a AG-50W × 8 (200–400 mesh) resin bed in 5 mL columns. For Rb measurements by MC-ICPMS, the Rb cut was further purified from Sr by a double pass with 3 M HNO_3 (Rb) and H_2O on Sr-Spec resin (50 μL) in 1 mL columns to reduce isobaric interferences from Sr at mass 87. Strontium isotope ratios were analysed statically on a VG AXIOM MC-ICPMS using methods described in detail by Waight et al. (2002a). Repeated analyses of the standard NBS 987 yielded 0.71025 ± 2 for $^{87}Sr/^{86}Sr$, with the external reproducibility having negligible effects on subsequent age calculations given the extremely radiogenic Sr of the mica samples. Rubidium isotope ratios for Rb concentration determinations were analysed by MC-ICPMS using admixed Zr to correct for Rb mass bias. Full details of Rb isotope dilution analysis are described in Waight et al. (2002b). Rb isotope ratios measured on synthetic standards reproduce to <0.1% and estimated total uncertainties on calculated mica Rb/Sr ratios are ±0.25%.

4.3. Pb isotopic analysis by LA-MC-ICPMS

Laser ablation Pb isotopic analysis of the rutile crystals was performed with a CETAC Nd-YAG (266 nm) laser coupled to a VG AXIOM MC-ICPMS. Analytical protocols that were followed are described in detail by Willigers et al. (2002), with two important exceptions: (1) the ^{201}Hg peak was used to correct for the presence of ^{204}Hg on ^{204}Pb—this is an important modification as use of either ^{200}Hg or ^{202}Hg yields an erroneously large 204 correction due to tungsten oxide interferences on masses 200 and 202 that are a function of the significant (approximately 100 ppb–1 ppm) trace quantities of tungsten in rutile. ^{201}Hg signals were typically <0.1 mV and result in corrections to the measured $^{204}Hg+^{204}Pb$ ion beam of <30%. (2) Rutile was ablated with a static laser beam (300–25 μm beam diameter – depending on crystal size) rather than a rastered ablation track, with analyses acquired over a number of 30 s periods (typically 3–5) as the laser progressively ablated a pit that was typically 0.1–0.2 mm deep into the rutile crystal. Even small rutile crystals are quite robust to ablation and may be ablated for up to 2 min with a laser beam not significantly smaller than the rutile diameter.

Only the largest rutile crystals could be ablated with a large enough laser beam to yield sufficiently large ^{204}Pb ion beams to permit measurement of $^{20x}Pb/^{204}Pb$ ratios using a Faraday collector to acquire the 204 ion beam. Thus, most analyses used the axial multiplier to acquire the 204-ion beam. All $^{207}Pb/^{206}Pb$ ratios were measured with Faraday collectors. Typical instrument sensitivity for a 50-μm laser beam diameter was 10 mV/ppm total Pb.

The NIST610 glass standard was used to correct the rutile Pb isotopic data for instrumental mass bias. The glass standard was run after every 1–5 unknown analyses (depending on the stability of the instrumental mass bias). Instrumental mass bias typically drifted ≪0.05% per atomic mass unit between standard analyses. Pb isotopic data for the rutile samples were corrected using the $^{208}Pb/^{206}Pb$ ratio measured on the NIST610 standard with respect to the precise double-spike Pb isotope determinations of this material by Baker et al. (2004) using the exponential mass fractionation law.

5. Results

5.1. Mica Rb–Sr ages

Table 1 presents new Rb–Sr data for seven mica samples that were collected in or near the site from which the rutile-bearing samples were taken. All the micas have radiogenic Sr compositions ($^{87}Sr/^{86}Sr = 2.85–85.25$) that permit calculation of two-point isochron ages from the two splits of mica analysed for most samples. This approach takes advantage of inter-crystal variations in mica Rb/Sr ratios to calculate ages although we acknowledge the ages may to some extent record internal equilibration with inclusions like apatite.

The single muscovite sample yields a two-point isochron age of 1485 ± 6 Ma, almost 100 Myr younger than the timing of peak metamorphism in the Reynolds Range. The two most magnesian phlogopites define two- and three-point isochron ages of 1454 ± 68 and 1411 ± 4 Ma, respectively (only one phlogopite split from KRN-6 was analysed) that are somewhat younger than the muscovite Rb–Sr age. In contrast, ages obtained from the less magnesian phlogopite and biotite from samples V91-4 (1352 ± 4 Ma), X-23 (984 ± 3 Ma), X-328 (807 ± 9 Ma) and X-372 (267 ± 19 Ma) are much younger than the high-*T*/low-*P* regional metamorphism of the Reynolds Range at ca. 1584 Ma. All of these samples appear to have suffered isotopic resetting during a later tectono-thermal event, presumably the 400–300 Ma Alice Springs orogeny. For the five samples exclusive of X-23, in which later alteration is clearly evident in the replacement of spinel by fine-grained corundum + magnetite ± chlorite, the susceptibility to isotopic resetting appears to be strongly related to the biotite composition. Initial Sr isotope ratios for the two-point mica "isochrons" vary from unrealistically low values to rather radiogenic values that, in part, probably reflect this later tectono-thermal event. The radiogenic initial Sr for the relatively young mica samples is generally consistent with resetting and the very high Rb/Sr ratio of the bulk samples.

In summary, while the mica Rb–Sr data record a complex history and multiple events, two salient points can be made: (1) the muscovite and most Mg-rich biotites

Table 1
Rb–Sr concentration and Sr isotope data for micas from Reynolds Range samples, with calculated Rb–Sr ages

Sample	Mineral	Mg/(Mg + Fe)[c]	Rb (ppm)	Sr (ppm)	$^{87}Rb/^{86}Sr$	$^{87}Sr/^{86}Sr$	Isochron age (Ma)[b]	Initial $^{87}Sr/^{86}Sr$
X-324	Muscovite	—	764.8	9.987	416.7	9.7243		
			466.8	12.205	145.7	3.9481	1485 ± 6	0.844 ± 0.017
X-14	Phlogopite	0.89	680.6	7.094	581.0	11.894		
	1.5 × 0.4 mm		531.1	5.367	625.1	12.815	1454 ± 68	−0.23 ± 0.60
KRN-6	Phlogopite	0.92	705.4	14.677	181.3	3.8227	1411 ± 4[a]	0.154 ± 0.016
	0.6 × 0.05 mm							
V91-4	Phlogopite	0.85	969.6	5.840	4451	85.2540		
	1.0 × 0.35 mm		864.7	6.523	4451	21.6720	1352 ± 4	−0.987 ± 0.085
X-23	Phlogopite	0.85	599.3	4.569	900.7	14.757		
	1.7 × 0.35 mm		478.5	14.560	124.1	3.829	984 ± 3	2.0835 ± 0.0070
X-328	Biotite	0.52	766.6	9.618	342.5	5.6755		
	0.75 × 0.15 mm		567.0	9.065	249.9	4.6091	807 ± 9	1.731 ± 0.037
X-372	Biotite	0.25	2520	22.169	397.6	2.8516		
	0.6 × 0.05 mm		2443	20.593	417.5	2.9272	267 ± 19	1.34 ± 0.11

[a] Three-point isochron of all phlogopite data (MSWD = 1.2) from X-14 and KRN-6.
[b] Isochron ages were calculated using: a reproducibility of 0.25% for the Rb/Sr ratio and an external reproducibility of 0.01% for $^{87}Sr/^{86}Sr$ ratios a ^{87}Rb decay constant of 1.42×10^{-11} yr^{-1} Steiger and Jäger (1977).
[c] Mg/(Mg + Fe total) measured by electron microprobe.

(phlogopite) record ages of ca. 1400–1500 Ma, with model ages using reasonable assumed initial Sr isotope ratios for the most radiogenic phlogopite recording ages slightly lower than the two-point isochron ages (1300–1350 Ma); (2) low-Mg phlogopite and biotite record much younger isochron (or model) ages that point to a young thermal overprint that exceeded the T_c for Sr in biotite.

5.2. Rutile Pb–Pb ages

The Pb isotopic data and calculated ages for the studied rutile samples are presented in Tables 2 and 3. Pb–Pb ages for the rutile can be calculated in a number of ways: (1) from the measured $^{207}Pb/^{206}Pb$ age with no correction for common Pb; (2) from every analysis using an assumed common Pb composition, for example a typical Proterozoic common Pb with $^{206}Pb/^{204}Pb$ and $^{207}Pb/^{204}Pb = 16.0$ and 15.3, respectively; (3) an isochron calculation from multiple analyses of the same rutile crystal—this isochron calculation can be performed with or without inclusion of a common Pb point. The composition of the common Pb point can be varied significantly without significantly affecting the calculated ages. All ages were calculated using the software of Ludwig (2000).

Pb–Pb ages calculated in these ways for 10 different rutile crystals from sample KRN-6 ranging in size from 3.5 to 0.6 mm are listed in Table 2. Ten Pb–Pb isochron ages using a common Pb point yield a mean age of 1544 ± 8 Ma and range in age from 1536.2 ± 3.5 to 1549.8 ± 1.7 Ma. Isochron ages calculated without a common Pb point are not significantly different (mean = 1550 ± 18 Ma; $n = 10$), but have larger uncertainties given that removal of the common Pb point reduces the spread on the isochron and results in a less precise age determination. Replicate single Pb–Pb ages, corrected for common Pb, on single crystals often reproduce to < ± 5 Myr. Interestingly, Pb–Pb ages calculated without correction for common Pb yield a mean age of 1549 ± 10 Ma ($n = 42$) that is within error of the Pb–Pb ages where a common Pb correction was performed. This reflects the small amounts of common Pb initially present in the rutile.

Given that the rutile from Reynolds Range contains insufficient common Pb to necessitate measuring ^{204}Pb and making a common Pb correction to obtain useful chronological data, the remaining samples were only analysed for their $^{207}Pb/^{206}Pb$ ratios. In the case of samples X-357, X-200, and X-195 this was unavoidable as we were unable to measure the 204 ion beam sufficiently precisely on these small crystals. Mean $^{207}Pb/^{206}Pb$ ages for these four samples and also different sized fractions from KRN-6 are given in Table 3. Despite a range in rutile size from >2.0 to 0.05 mm there is little evidence for a systematic relationship between crystal size and age (Table 3) amongst the different populations of rutile, which have mean ages within the extremes defined by samples X-200 (1517 ± 42 Ma; $n = 9$) and X-327 (1560 ± 26 Ma; $n = 18$). It should be acknowledged that the observation that the ^{207}Pb–^{206}Pb ages concur with Pb–Pb ages corrected for common Pb is based only on sample KRN-6. As such, it is possible that some of the ages determined on smaller rutile are an overestimate. However, we monitored 204 during all the analyses and $^{206}Pb/^{204}Pb$ ratios for small rutile were always >10,000 (with large errors)—not correcting for these levels of common Pb would only constitute a 1% over-estimation of the ^{207}Pb–^{206}Pb ages for the small rutile crystals.

In summary, all the rutiles dated in this study define a relatively restricted range of ages (mean = 1543 Ma) that is only ca. 40 Myr younger than the peak metamorphic event (1584 Ma; ⩾750 °C) that affected the Reynolds Range samples as recorded by zircon and monazite Pb–Pb dating. The rutile ages are ca. 60 Myr older than the muscovite Rb–Sr age and >100 Myr older than the

Table 2
LA-MC-ICPMS Pb isotope determinations and age calculations for rutile from sample KRN-6

Rutile crystal	204 collector[a]	Spot size (μm)	Crystal size (mm) (diameter)	$^{206}Pb/^{204}Pb$	%SE	$^{207}Pb/^{204}Pb$	%SE	$^{207}Pb/^{206}Pb$	%SE	$^{207}Pb/^{206}Pb$ age (Ma)[b]	Error 2 SD	Pb–Pb age (common Pb corrected) (Ma)[c]	Error 2 SD	Pb–Pb isochron age (without common Pb) (Ma)[d]		MSWD	*n*	Pb–Pb isochron age (with common Pb) (Ma)		MSWD	*n*
KRN-6 (21)	F	300	3.5	7760	8.3	758	8.1	0.097103	0.097	1569.2	2.3	1545	4								
				28446	7.8	2744	7.8	0.096288	0.023	1553.4	0.5	1547	4								
				27748	30.9	2674	30.8	0.096265	0.026	1552.9	0.6	1546	17								
				21639	33.8	2088	33.7	0.096264	0.025	1552.9	0.6	1545	18	1547.7	± 5.8	0.0	4	1546.0	± 3.0	0.2	5
KRN-6 (21)	EM	300	3.5	39386	6.1	3785	6.1	0.096055	0.027	1548.9	0.6	1543	3								
				43430	6.5	4184	6.5	0.096158	0.039	1550.9	0.9	1548	4								
				35606	34.2	3422	34.2	0.096060	0.020	1549.0	0.5	1542	19								
				42539	26.7	4085	26.7	0.096084	0.024	1549.5	0.6	1542	14					1545	± 11	1.8	5
KRN-6 (2)	F	300	2.0	7732	11.0	752	10.9	0.095878	0.048	1545.4	1.1	1537	6								
				34041	7.9	3261	7.9	0.095725	0.015	1542.3	0.3	1536	4	1535.2	± 5.9	–	2	1536.2	± 3.5	0.1	3
KRN-6 (2)	EM	300	2.0	48413	5.4	4638	5.4	0.095788	0.017	1543.6	0.4	1538	3								
				34875	23.0	3340	23.0	0.095725	0.011	1542.3	0.3	1536	13								
				31390	23.8	3001	23.9	0.095710	0.019	1542.0	0.4	1531	15	1549	± 21	0.1	3	1537.8	± 2.8	0.6	4
KRN-6 (11)	EM	300	1.9	43900	5.0	4226	5.0	0.096208	0.022	1551.8	0.5	1547	3								
				53808	7.3	5169	7.3	0.095975	0.017	1547.3	0.4	1544	4								
				13653	50.5	1306	50.5	0.095647	0.010	1540.9	0.2	1521	33	1553	± 68	3.4	3	1547	± 20	2.3	4
KRN-6 (28)	EM	300	1.8	34646	3.3	3336	3.3	0.096199	0.012	1551.6	0.3	1546	2								
				54965	5.4	5282	5.4	0.096097	0.010	1549.7	0.2	1545	3								
				59337	6.7	5697	6.7	0.096042	0.010	1548.6	0.2	1543	4								
				72478	5.9	6960	5.9	0.095994	0.012	1547.7	0.3	1545	3	1542.5	± 4.9	0.3	4	1545.1	± 1.3	0.6	5
KRN-6 (27)	EM	300	1.4	32295	4.1	3107	4.1	0.096075	0.020	1549.3	0.5	1544	2								
				42057	5.1	4033	5.1	0.095881	0.010	1545.4	0.2	1539	3								
				53116	5.0	5101	5.0	0.096088	0.015	1549.5	0.3	1544	3								
				51575	4.8	4951	4.8	0.096048	0.017	1548.7	0.4	1543	3	1544	± 27	3.5	4	1542.6	± 6.3	2.4	5
KRN-6 (31)	EM	300	1.2	38293	3.3	3667	3.3	0.095691	0.015	1541.6	0.3	1536	2								
				42692	3.7	4099	3.7	0.096028	0.013	1548.4	0.3	1542	2								
				52818	3.7	5075	3.7	0.096084	0.014	1549.5	0.3	1544	2								
				49408	4.3	4745	4.3	0.096037	0.017	1548.5	0.4	1543	2	1565.3	± 9.5	1.1	4	1543	± 11	14.0	5
KRN-6 (25)	EM	300	1.1	43835	3.7	4213	3.7	0.096061	0.011	1549.0	0.3	1544	2								
				58100	4.9	5584	4.9	0.096075	0.012	1549.3	0.3	1545	3								
				41346	3.6	3972	3.6	0.096062	0.011	1549.0	0.3	1542	2								
				52051	4.3	4992	4.3	0.095911	0.011	1546.0	0.3	1541	2	1548	± 40	3.9	4	1543.6	± 7.5	2.7	5
KRN-6 (91)	EM	200	1.1	24190	29.9	2335	29.9	0.096471	0.012	1557.0	0.3	1547	17								
				69657	5.9	6714	5.9	0.096363	0.017	1554.9	0.4	1552	3								
				63908	4.9	6155	4.9	0.096292	0.015	1553.4	0.3	1550	3								
				75520	5.8	7267	5.8	0.096227	0.015	1552.1	0.3	1549	3	1550.8	± 8.6	0.9	4	1549.8	± 1.7	0.6	5
KRN-6 (100)	EM	200	0.6	77788	4.6	7479	4.6	0.096097	0.016	1549.7	0.4	1547	2								
				36213	24.3	3477	24.3	0.096064	0.018	1549.1	0.4	1541	13								
				61164	15.2	5869	15.2	0.095949	0.017	1546.8	0.4	1543	8	1554	± 12	0.5	3	1546.6	± 2.2	1.0	4
KRN-6 (131)	EM	200	0.6	23817	29.8	2280	27.0	0.095726	0.023	1542.4	0.5	1531	99								
				24507	19.4	2347	19.4	0.095787	0.018	1543.5	0.4	1532	11								
				35157	5.5	3379	5.5	0.096122	0.025	1550.2	0.6	1542	3	1565	± 32	0.0	3	1541.3	± 3.0	1.8	4

[a] F, Faraday collector; EM, electron multiplier.
[b] Pb–Pb age calculated without correction for common Pb.
[c] Using a common Pb composition of $^{206}Pb/^{204}Pb = 16.5$ and $^{207}Pb/^{204}Pb = 15.3$ (±1%).
[d] Calculated with rho estimated as being 0.9999 (Willigers et al., 2002).

Table 3
Mean ^{207}Pb–^{206}Pb ages (not corrected for common Pb) calculated for samples from KRN-6 (Table 1 and additional data) and four other additional rutile-bearing samples from the Reynolds Range

Sample	Crystal size (mm)	Pb–Pb age (Ma)[a]	Error 2SD	*n*	Lowest Pb–Pb age (Ma)
KRN-6	⩾2.0	1548	±16	68	1530
	1.0–2.0	1549	±10	44	1539
	0.5–1.0	1544	±7	16	1539
	<0.5	1545	±15	17	1539
X-16	0.75	1552	±14	19	1538
X-357	0.20	1560	±26	18	1536
X-200	0.10	1517	±42	9	1491
X-195	0.05	1538	±17	10	1531

[a] Pb–Pb age calculated without correction for common Pb.

phlogopite and biotite Rb–Sr ages. Even the smallest rutile crystals show no apparent evidence of the isotopic resetting that affected the Rb–Sr system in some phlogopite and all biotite samples from the Reynolds Range.

6. Discussion

6.1. Effective diffusion radius for rutile

As discussed earlier in section 2.0, textural evidence clearly demonstrates that the rutile studied here is a peak metamorphic mineral that is neither detrital nor a secondary recrystallization product formed during local hydrothermal fluid flow and reheating. It is also important to establish that Pb in the rutile behaved according to the principals of volume diffusion that enable a rigorous comparison of different chronometers. The latter point is particularly important given the apparent lack of a relationship between age and rutile crystal size. For the rutile sizes analysed here, a difference in T_c of nearly 200 °C, corresponding to age differences of 100–70 Myr, would be expected (see Fig. 4) based on the results of experimental studies of Pb diffusion in rutile (Cherniak, 2000).

The apparent lack of a relationship between Pb–Pb age and crystal size can be readily be explained as a result of the sampling protocol adopted in this study. Although it is possible that for the very smallest rutiles, for which we did not perform a common Pb correction, the apparent ages could be 10–39 Myr too old, masking the effects of volume diffusion, the LA analyses only sample the outer 0.1–0.2 mm of crystals. The effective diffusion radius for the dated material in the large and small crystals should be comparable, and thus there is no evidence to suggest that Pb in rutile was not following volume diffusion laws.

6.2. Closure temperature for diffusion of Pb in rutile

The results of a recent experimental study indicate that rutile has a much higher T_c for Pb diffusion than previously thought (>ca. 600 °C for rutile grains larger than about 0.2 mm in diameter (Cherniak, 2000), versus ca. 400 °C for grains 0.2 mm in diameter and cooling rates of ca. 1 °C/Myr (Mezger et al., 1989a)). Furthermore, rutile is chemically simple (almost pure TiO_2), does not undergo exsolution during cooling, is resistant to low temperature alteration in most geologic environments, and the available experimental and empirical results indicate that the activation energy for Pb diffusion in rutile is quite high (242 ± 10 kJ/mol (Cherniak, 2000); 167–293 kJ/mol (Mezger et al., 1989a)). Rutile should therefore be a robust high temperature geochronometer that is little affected by subsequent isotopic resetting. The results from the study area confirm these general interpretations, with the first order observation that even the smallest rutile crystals (0.05 mm) record Pb–Pb ages some 60–130 Myr *older* than both the muscovite and the most phlogopitic mica Rb–Sr ages, supporting the interpretation that the T_c for Pb diffusion in rutile is well in excess of 550 and 435 °C, respectively.

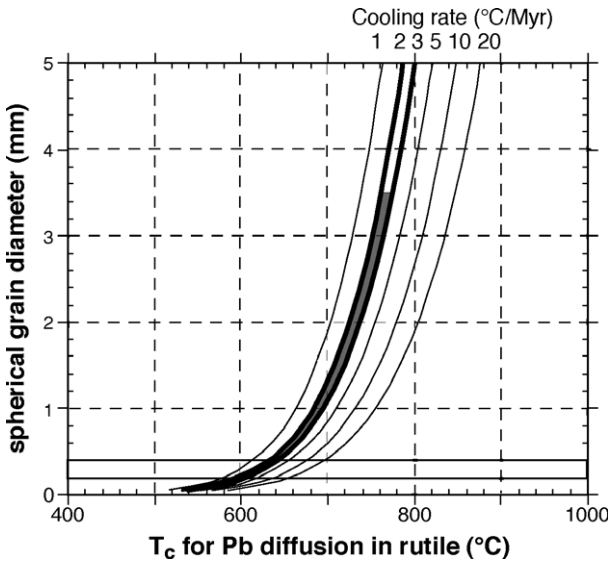

Fig. 4. Dependency of Pb diffusion in rutile as a function of grain size and cooling rate based on the experimental work of Cherniak (2000) i.e., $D = 1.55 \times 10^{-10} \times \exp(-242 \pm 10\ \text{kJ mol}^{-1}/\text{RT})\ \text{m}^2\ \text{s}^{-1}$. The bold curves indicate the inferred cooling rate for the study area, providing a T_c of 780–530 °C (shaded) for the studied rutile crystals that are 3.5–0.05 mm in diameter. The solid horizontal lines show the range of effective grain diameters for the sampling protocols used in this study.

In considering the closure temperature for rutile, it is useful to be able to compare age results previously obtained from associated zircon and monazite. The behaviour of zircon and monazite in response to metamorphism in the Reynolds Range is well understood, mainly through the work of Rubatto et al. (2001). Despite the long slow cooling history, monazite and metamorphic zircon from granulite facies rocks in the SE Reynolds Range give similar ages, with weighted mean ages approximately 35 Myr older than those for the rutile studied here (Fig. 3). That a trace of inheritance remains, rarely, in some of the monazite from this region indicates that the closure temperature of the U–Pb system in the monazite crystals, which are typically relatively small (0.05–0.2 mm diameter) can exceed 750–800 °C (Vry et al., 1996; Rubatto et al., 2001).

Over the past two decades the closure temperatures for many geochronometers, especially higher temperature geochronometers, have been revised upwards (Willigers et al., 2001). While earlier estimates of the closure temperature of the U–Pb system in monazite were ~600–750 °C (Copeland et al., 1988; Parrish, 1990; Mezger et al., 1991; Smith and Giletti, 1997), later studies (e.g., Spear and Parrish, 1996; Kamber et al., 1998) have shown that the T_c must be higher than 700–750 °C. A $T_c \geqslant 800$ °C (Kamber et al., 1998) appears reasonably consistent with the Reynolds Range data (Vry et al., 1996; Williams et al., 1996; Rubatto et al., 2001). Even higher closure temperatures, in excess of 900 °C, have been suggested for monazite (Schmitz and Bowring, 2003; Cherniak et al., 2004), but there is little evidence to support them in the Reynolds Range, where inheritance in monazite is very uncommon.

Fig. 4 shows the curves for T_c for Pb diffusion in rutile at different cooling rates (Cherniak, 2000), with the T_c range (shaded) for natural rutile grains ($\leqslant$3.5 mm in size) from the present study area. The bold curves on Fig. 4 indicate the approximate cooling rate for the study area, based on the results of this and earlier studies (see Fig. 5). The experimental results (Cherniak, 2000) indicate that the T_c for Pb diffusion in relatively large ($\geqslant$2 mm) rutile crystals from the Reynolds Range (Fig. 4) should be comparable to the temperatures at which new zircon rims can grow ($\geqslant$ca. 700 °C; e.g., Rubatto et al., 2001). Fig. 3 shows that instead, the analysed rutile records a lower closure temperature. This is the expected result; the LA analyses only sample the outer 0.1–0.2 mm of the larger crystals and as such the diffusion domain of the dated material should be comparable to that of much smaller crystals (ca. 0.2–0.4 mm diameter, for rounded, nearly spherical crystals). The horizontal lines near the base of Fig. 4 delimit the range of effective grain diameters for the sampling protocols used in the present study. Based on the experimental results, the effective closure temperature for rutile cooled at 2–3 °C/Myr and analysed by the LA-MC-ICPMS method described here should be near 620 °C. This is in excellent agreement with the T_c of 630 °C that is obtained based on the previous estimates of peak metamorphism at 1584 Ma and ca. 750 °C, followed by cooling at 3 °C/Myr, and a rutile age of 1544 Ma.

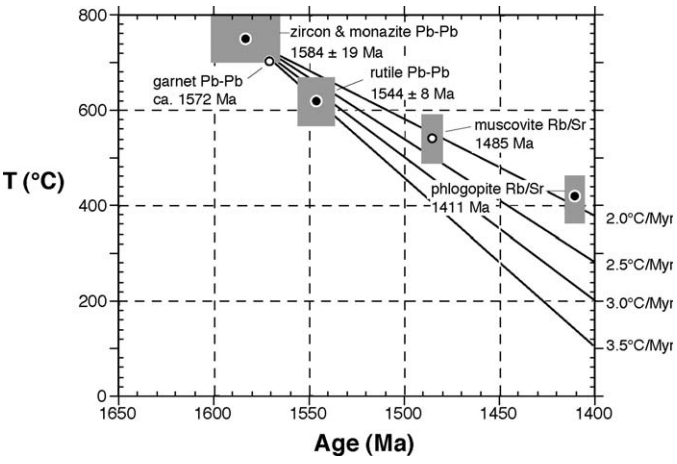

Fig. 5. Cooling history of high-grade metamorphic rocks from the Reynolds Range. Solid circles, age constraints from this study area i.e., zircon and monazite (Vry et al., 1996); open circles, age constraints from elsewhere in the Reynolds Range i.e., garnet in late-stage veins (Buick et al., 1999). Rb–Sr age results from this study for muscovite and phlogopite (Table 1) are also plotted.

Given that the earlier empirical calibration of Mezger et al. (1989a) suggested that the T_c for Pb diffusion in rutile was relatively low (ca. 400 °C) it is pertinent to briefly consider why that pioneering study of rutile Pb–Pb dating apparently yielded different results to those presented here. Mezger et al. (1989a) analysed small rutile crystals from the Proterozoic Adirondack terrane (New York, USA) and the Archaean Pikwitonei granulite domain at Cauchon Lake in Manitoba, Canada. Based on their results, they proposed that T_c for Pb diffusion in rutile was ca. 380 °C for rutile grains that were 0.14–0.18 mm in size, and ca. 420 °C for grains about 0.18–0.42 mm in size. Even for small grain sizes, these are much lower than either the experimental results of Cherniak (2000) or the present study would indicate. The reason for this discrepancy seems to be relatively straightforward. Mezger et al. (1989a) constructed a T–t path for the Adirondack Highlands based on the following chronometers and closure temperatures: (1) U–Pb in monazite (650–700 °C); (2) U–Pb in sphene (680–500 °C); (3) Ar in hornblende (400–450 °C) and (4) Ar in biotite (ca. 300 °C). However, estimates of closure temperatures for these (and many other chronometric systems) are now generally believed to be considerably higher (cf. Willigers et al., 2004), and the following closure temperatures would perhaps be more appropriate for the constructing the T–t history of the Adirondack Highlands: (1) U–Pb in monazite ($\geqslant$800 °C; Kamber et al., 1998); (2) U–Pb in sphene (670 ± 45 °C; Cherniak, 1993; Mezger et al., 1993); (3) Ar in hornblende (580 °C; Cherniak et al., 1991; Kamber et al., 1995); and (4) Ar in biotite (ca. 400 °C; Verschure et al., 1980; Del Moro et al., 1982; Harrison et al., 1985). Using these closure temperature estimates, we calculate a T_c for Pb diffusion in the rutile from the study of Mezger et al. (1989a) to be 500 °C and 540 °C for rutile with a diameter of 0.14–0.18 and 0.18-0.42 mm, respectively. These estimates are ca. 120 °C higher than those quoted by Mezger et al. (1989a). Considering the small grain size of the rutile from the study of Mezger et al., and the slow cooling rate ($\leqslant$1 °C/Myr) of the Adirondack terrane this re-interpretation of the age data in Mezger et al. (1989a) is in close agreement with the results of this study and also the experimental work of Cherniak (2000) (Fig. 4). Mezger et al. (1989a) also Pb–Pb dated rutile from the Archaean Pikwitonei granulite terrane and obtained ages for rutile ca. 0.12–0.40 mm in size that overlap and extend to slightly younger ages than K–Ar ages for hornblende from the same terrane. This suggests that the larger rutile crystals from the Pikwitonei granulites have a T_c close to 580 °C, again in excellent agreement with

the interpretation that rutile has a high and not low T_c for Pb diffusion.

In summary, the results of both this study and a recent experimental study (Cherniak, 2000) indicate that the Pb–Pb system in rutile should function as a high-temperature geochronometer that is resistant to later isotopic reequilibration. The LA-MC-ICPMS method described here samples only the outer 0.1–0.2 mm of the rutile crystals, giving a grain size independent apparent T_c for Pb diffusion in rutile of ca. 620 °C. It is important to note that the potential uncertainty on the ^{87}Rb decay constant (e.g., Begemann et al., 2001) would not affect the interpretation that rutile has a high T_c for Pb diffusion in rutile. For example, if the ^{87}Rb decay constant is 1.40×10^{-11} yr^{-1}, as has been suggested by Begemann et al. (2001), the mica ages on Fig. 5 would be translated to ages that are ca. 20 Myr older—this would only place the mica Rb–Sr ages closer to the 2.5 °C/Myr cooling curve, with no significant effect on the T_c estimates for rutile.

In conclusion, neither the chronological study of rutile from the Reynolds Range presented herein or the experimental study of Cherniak (2000) are consistent with the historical use of rutile as a low-temperature (ca. 400 °C) geochronometer to provide constraints on metamorphic cooling. We suggest that the closure temperatures quantified by Cherniak (2000) should be adopted when constructing T–t histories for metamorphic terranes.

6.3. Slow cooling in high-T/low-P metamorphic terranes

High-T/low-P metamorphism is a feature of the geological history of Proterozoic Australia, including not only the Reynolds Range region but also, for example, the Halls Creek Orogen (Bodorkos et al., 2002) and the Mount Isa Inlier, where high temperatures apparently lasted 100 Ma (McLaren et al., 1999). The Reynolds Range underwent prolonged slow cooling at ca. 3 °C/Myr following the peak of regional granulite-facies metamorphism at ca. 1584 Ma (Williams et al., 1996; Buick et al., 1998, 1999; Rubatto et al., 2001). The zircon, monazite and garnet Pb–Pb ages that were used to help constrain that T–t history are shown in Figs. 3 and 5. The new rutile data add to that dataset, and show that the slow cooling persisted for ca. 40 Myr, 10–15 Myr longer than previously recognised (Fig. 5). For such high temperatures to persist for 40 Myr at shallow crustal levels (mostly $\leqslant$4 kbar; Vry and Cartwright, 1994; Buick et al., 1998) requires that the high-T/low-P regional metamorphism and subsequent cooling took place on a relatively high geotherm that reached a nearly steady state (Williams et al., 1996; Buick et al., 1998, 1999; Sandiford and Hand, 1998; McLaren et al., 1999; Rubatto et al., 2001). As discussed by Buick et al. (1998), this is unlikely to have resulted from either advective heating by granite magmas, crustal thickening and/or synchronous mantle thinning. Rather, it seems likely that the thermal history of this terrane reflects conductive heating resulting from burial of a layer of material characterised by anomalously high heat production, like the abundant, anomalously high heat-producing granites that occur in the Reynolds Range (Loosveld, 1989; Chamberlain and Sonder, 1990; Buick et al., 1998; Sandiford and Hand, 1998; Hand et al., 1999). If so, the terrane would be expected to remain at high temperatures for long periods, and the persistent low-P/high-T metamorphism should only be terminated by decompression (Sandiford and Hand, 1998). Further work will be needed to ascertain whether burial of a layer of U- and Th-enriched granites can explain the lateral temperature gradients recorded by metamorphic grades exposed at approximately the same crustal level in the field area. Nonetheless, our results are fully consistent with past suggestions that the high-T/low-P metamorphism in the Reynolds Range took place on a conductive geotherm, under nearly steady-state conditions.

6.4. Extending the T–t history of the Reynolds Range to lower temperatures

To use the new mica data to extend the previously constrained T–t path for the Reynolds Range to low temperatures first requires some assessment of the closure temperature of the Rb–Sr system in different micas. Closure in mica Rb–Sr systems depends on numerous factors, including grain size, modal mineralogy, Rb and Sr diffusion coefficients, and Rb and Sr contents of co-existing phases and their partition coefficients (Jenkin et al., 1995, 2001). In preparing Fig. 5, a T_c of ca. 550 °C for Sr in muscovite was used (e.g., Jenkin, 1997; Inger, 1998). In constraining the lower temperature portions of the regional cooling history (Fig. 5) we have assumed that closure of the Rb–Sr system in the large phlogopite-rich crystals occurred at ca. 435 °C (Willigers et al., 2004). Trioctahedral micas with lower phlogopite contents than sample X-14 and KRN-6 give anomalously low Rb–Sr ages, commonly between about 1000 and 800 Ma, but as low as 267 Ma, for the samples that we have analysed (Table 1). The younger Rb–Sr ages apparently record the decreasing T_c in the less phlogopitic micas. The closure temperature for biotite is likely to be ca. 400 °C, but the variable isotopic resetting precludes using any but the most phlogopitic compositions to construct the Proterozoic T–t path for the Reynolds Range.

The limited amount of new mica Rb–Sr data obtained in this study greatly extends the previous thermal history to lower temperatures, and hints at a much later tectonothermal event that reset some mica ages. Most of the young biotite Rb–Sr ages are interpreted to reflect partial isotopic resetting during the 400–300 Ma Alice Springs orogeny when thick-skinned, south-directed, intraplate deformation thrust Arunta Inlier basement over the northern margin of the Amadeus Basin (Teyssier, 1985; Shaw et al., 1991, 1992; Dunlap and Teyssier, 1995). A few biotite samples have given even lower (Permian to Triassic) Rb–Sr ages, the cause of which is unknown.

The mica results are interpreted as preliminary evidence that slow cooling at ca. 2–3 °C/Myr may have persisted for nearly 200 Myr following the metamorphic peak. If so, the Reynolds Range may record the longest period of slow cooling at shallow depths documented to date.

6.5. Pb–Pb dating of rutile by MC-ICPMS

Willigers et al. (2002) showed that it was possible to rapidly Pb–Pb date apatite, sphene and monazite by LA-MC-ICPMS analysis. This study has extended the versatility of this method to rutile, which in this study has a considerably lower Pb content (ca. 20 ppm) than the minerals dated by Willigers et al. (2002). Single rutile grains down to 0.5 mm in size can be readily Pb–Pb dated, including correction for common Pb, to a precision that is typically much better than ±0.5%. This uncertainty is based on the typical uncertainty of individual rutile isochron ages (calculated with a common Pb point) and is also comparable to the reproducibility of the 12 ages determined on rutile from KRN-6. Smaller rutile grains can only be ^{207}Pb–^{206}Pb dated as our instrument set-up lacks the sensitivity to precisely measure the 204 ion beam in smaller grains. A brief review of rutile Pb contents, Pb isotope compositions, and μ values ($^{238}U/^{204}Pb$ values) from the literature indicates that with the probable exception of rutile from certain eclogites (e.g., Di Vincenzo et al., 1997; Treloar et al., 2003) rutile from a variety of metapelitic and metamorphosed igneous rocks (cf. Mezger et al., 1989a,b, 1991; Miller et al., 1996; Davis, 1997; Indares and Dunning, 2001; Timmermann et al., 2004) should be amenable to analysis by the LA-MC-ICPMS method described here.

7. Conclusions

We have demonstrated for the first time that LA-MC-ICPMS can be used to rapidly obtain relatively precise Pb–Pb age determinations ($\leqslant \pm 0.5\%$) from natural rutile crystals. The LA-MC-ICPMS method described here samples only the outer 0.1–0.2 mm of the rutile crystals, giving a grain size independent apparent closure temperature (T_c) for Pb diffusion in rutile of ca. 620 °C—less than that of monazite ⩽0.1 mm in diameter, but significantly higher than the Rb–Sr system in muscovite (550 °C), phlogopite (435 °C) and biotite (400 °C), for rocks cooled at 2–3 °C/Myr. This conclusion is in accordance with results of recent experimental work by Cherniak (2000), and with current T_c estimates for monazite and other high temperature geochronometers, which have been revised upwards in recent years.

The new rutile ages, together with the other geochronological data from the region, support the interpretation that the Reynolds Range, a classic high-*T*/low-*P* metamorphic belt in central Australia, underwent prolonged slow cooling on a conductive geotherm, under nearly steady-state conditions. Slow cooling at ca. 3 °C/Myr continued for at least 40 Myr following the peak of regional granulite-facies metamorphism at ca. 1584 Ma, and may have persisted at 2–3 °C/Myr for 200 Myr overall.

Acknowledgments

This study was funded by the Danish Lithosphere Centre (DLC) which receives its funding from the Danish National Research Foundation. J.K.V. gratefully acknowledges the receipt of travel funding from the Royal Society of New Zealand International Science and Technology Linkages Programme (funding from the Ministry of Science, Research and Technology). J.K.V. thanks the people at the DLC for the opportunity to visit the DLC and to actively partake in collaborative research there, and also for their many kindnesses during her visit. Tod Waight is particularly thanked for the knowledgeable guidance and assistance he provided to J.K.V. in aspects of the analytical work, and especially for his assistance in the MC-ICPMS laboratory. We thank Yuri Amelin, Paul Sylvester, Fernando Corfu and an anonymous reviewer for their helpful comments, which improved the manuscript.

Associate editor: Yuri Amelin

References

Baker, J.A., Peate, D.W., Waight, T.E., Meyzen, C., 2004. High-precision Pb isotopic analysis of standards and samples using thallium and a lead double spike with a double focusing MC-ICPMS. *Chem. Geol.* **211**, 275–303.

Begemann, F., Ludwig, K.R., Lugmair, G.W., Min, K., Nyquist, L., Patchett, P.J., Renne, P.R., Shih, C.Y., Villa, I.M., Walker, R.J., 2001. Call for an improved set of decay constants for geochronological use. *Geochim. Cosmochim. Acta* **65**, 111–121.

Bodorkos, S., Sandiford, M., Oliver, N.H.S., Cawood, P.A., 2002. High-T, low-P metamorphism in the Palaeoproterozoic Halls Creek Orogen, northern Australia: the middle crustal response to a mantle-related transient thermal pulse. *J. Metamorph. Geol.* **20**, 217–237.

Buick, I.S., Cartwright, I., Harley, S.L., 1998. The retrograde *P–T–t* path for low-pressure granulites from the Reynolds Range, central Australia: petrological constraints and implications for low-P/high-T metamorphism. *J. Metamorph. Geol.* **16**, 511–529.

Buick, I., Frei, R., Cartwright, I., 1999. The timing of high-temperature retrogression in the Reynolds Range, central Australia: constraints from garnet and epidote Pb–Pb dating. *Contrib. Mineral. Petrol.* **135**, 244–254.

Chamberlain, C.P., Sonder, L.J., 1990. Heat-producing elements and the thermal and baric patterns of metamorphic belts. *Science* **250**, 763–769.

Cherniak, D.J., Lanford, W.A., Ryerson, F.J., 1991. Lead diffusion in apatite and zircon using ion implantation and Rutherford backscattering techniques. *Geochim. Cosmochim. Acta* **55**, 1663–1673.

Cherniak, D.J., 1993. Lead diffusion in titanites and preliminary results on the effects of radiation damage on Pb transport. *Chem. Geol.* **110**, 177–194.

Cherniak, D.J., 2000. Pb diffusion in rutile. *Contrib. Mineral. Petrol.* **139**, 198–207.

Cherniak, D.J., Watson, E.B., Grove, M., Harrison, T.M., 2004. Pb diffusion in monazite: a combined RBS/SIMS study. *Geochim. Cosmochim. Acta* **68**, 829–840.

Copeland, P., Parrish, R.R., Harrison, T.M., 1988. Identification of inherited radiogenic Pb in monazite and its implications for U–Pb systematics. *Nature* **333**, 760–763.

Davis, W.J., 1997. U–Pb zircon and rutile ages from granulite xenoliths in the Slave province: evidence for mafic magmatism in the lower crust coincident with Proterozoic dike swarms. *Geology* **25**, 343–346.

Del Moro, A., Puxeddu, M., Radicati di Brozolo, F., Villa, I.M., 1982. Rb–Sr and K–Ar ages on minerals at temperatures of 300–400 °C from deep wells in the Larderello geothermal field (Italy). *Contrib. Mineral. Petrol.* **81**, 340–349.

Di Vincenzo, G., Palmeri, R., Talarico, F., Andriessen, P.A.M., Ricci, C.A., 1997. Petrology and geochronology of eclogites from the Lanterman Range, Antarctica. *J. Petrol.* **38**, 1391–1417.

Dunlap, W.J., Teyssier, C., 1995. Paleozoic deformation and isotopic disturbance in the southeastern Arunta Block, central Australia. *Precambrian Res.* **71**, 229–250.

Hand, M., Slater, K., MacLaren, S., Sandiford, M., 1999. Heat production rates in Australian Proterozoic terrains. *Geological Society of Australia* Abstracts No. 54, p. 35.

Harrison, T.M., Duncan, I., McDougall, I., 1985. Diffusion of ^{40}Ar in biotite: temperature, pressure and compositional effects. *Geochim. Cosmochim. Acta* **50**, 2461–2468.

Heaman, L., Parrish, R., 1991. U–Pb geochronology of accessory minerals. In: Heaman, L., Ludden, J.N. (Eds.), *Applications of Radiogenic Isotope Systems to Problems in Geology*. Min. Assoc. Canada, Short Course Handbook, Ottawa, pp. 59–102.

Indares, A., Dunning, G., 2001. Partial melting of high-*P*–*T* metapelites from the Tshenukutish Terrane (Grenville Province): petrography and U–Pb geochronology. *J. Petrol.* **42**, 1547–1565.

Inger, S., 1998. Timing of an extensional detachment during convergent orogeny: New Rb–Sr geochronological data from the Zanskar shear zone, northwestern Himalaya. *Geology* **26**, 223–226.

Jenkin, G.R.T., 1997. Do cooling paths derived from mica Rb–Sr data reflect true cooling paths? *Geology* **25**, 907–910.

Jenkin, G.R.T., Rogers, G., Fallick, A.E., Farrow, C.M., 1995. Rb–Sr closure temperatures in bi-minerallic rocks: a mode effect and test for different diffusion models. *Chem. Geol.* **122**, 227–240.

Jenkin, G.R., Ellam, R.M., Rogers, G., Stuart, F., 2001. An investigation of closure temperature of the biotite Rb–Sr system: the importance of cation exchange. *Geochim. Cosmochim. Acta* **65**, 1141–1160.

Kamber, B.S., Kramers, J.D., Napier, R., Cliff, R.A., Rollinson, H.R., 1995. The Triangle Shearzone, Zimbabwe, revisited: new data document an important event at 2.0 Ga in the Limpopo Belt. *Precambrian Res.* **70**, 191–213.

Kamber, B.S., Frei, R., Gibb, A.J., 1998. Pitfalls and new approaches in granulite chronometry. An example from the Limpopo Belt, Zimbabwe. *Precambrian Res.* **91**, 269–285.

Loosveld, R.J.H., 1989. The synchronism of crustal thickening and high T/low P metamorphism of the Mt. Isa inlier, Australia. II. Fast convective thinning of mantle lithosphere during crustal thickening. *Tectonophysics* **165**, 191–218.

Ludwig, K., 2000. Isoplot/Ex. Version 1.00 A geochronological toolkit for Microsoft Excel, BGC Publication 1.

McLaren, S., Sandiford, M., Hand, M., 1999. High radiogenic heat-producing granites and metamorphism—an example from the western Mount Isa inlier, Australia. *Geology* **27**, 679–682.

Mezger, K., Hanson, G.N., Bohlen, S.R., 1989a. High precision U–Pb ages of metamorphic rutile: applications to the cooling history of high-grade terranes. *Earth Planet. Sci. Lett.* **96**, 106–118.

Mezger, K., Hanson, G.N., Bohlen, S.R., 1989b. U–Pb systematics of garnet: dating the growth of garnet in the Late Archean Pikwitonei granulite domain at Caucon and Natawahunan Lakes, Manitoba, Canada. *Contrib. Mineral. Petrol.* **101**, 136–148.

Mezger, K., Rawnsley, C., Bohlen, S., Hanson, G., 1991. U–Pb garnet, sphene, monazite, and rutile ages: implications for the duration of high-grade metamorphism and cooling histories, Adirondack Mountains, New York. *J. Geol.* **99**, 415–428.

Mezger, K., van der Pluijm, B.A., Essene, E.J., Halliday, A.N., 1993. Thermochronology of the southern Grenville Orogen in Ontario, Canada. *Contrib. Mineral. Petrol.* **114**, 13–26.

Miller, B.V., Dunning, G.R., Barr, S.M., Raeside, R.P., Jamieson, R.A., Reynolds, P.H., 1996. Magmatism and metamorphism in a Grenvillian fragment: U–Pb and ^{40}Ar/^{39}Ar ages from the Blair River Complex, northern Cape Breton Island, Nova Scotia, Canada. *GSA Bull.* **108**, 127–140.

Parrish, R.R., 1990. U–Pb dating of monazite and its application to geological problems. *Can. J. Earth Sci.* **27**, 1431–1450.

Rubatto, D., Williams, I.S., Buick, I.S., 2001. Zircon and monazite response to prograde metamorphism in the Reynolds Range, central Australia. *Contrib. Mineral. Petrol.* **140**, 458–468.

Sandiford, M., Hand, M., 1998. Australian Proterozoic high temperature, low pressure metamorphism on the conductive limit. In: Treloar, P.J., O'Brien, P.J. (Eds.), *What Drives Metamorphism and Metamorphic Reactions?* Geol. Soc. Lond. Spec. Publ., London, pp. 109–120.

Santos Zalduegui, J.F., Schärer, U., Gil Ibarguchi, J.I., Girardeau, J., 1996. Origin and evolution of the Paleozoic Cabo Ortegal ultramafic–mafic complex (NW Spain): U–Pb, Rb–Sr, and Pb–Pb isotope data. *Chem. Geol.* **129**, 281–304.

Schmitz, M.D., Bowring, S.A., 2003. Ultrahigh-temperature metamorphism in the lower crust during Neoarchean Ventersdorp rifting and magmatism, Kaapvaal Craton, southern Africa. *G.S.A. Bull.* **115**, 533–548.

Shaw, R.D., Etheridge, M.A., Lambeck, K., 1991. Development of the Late Proterozoic to mid-Palaeozoic, intracratonic Amadeus Basin in central Australia: a key to understanding tectonic forces in plate interiors. *Tectonics* **4**, 688–721.

Shaw, R.D., Zeitler, P.K., McDougall, I., Tingate, P.R., 1992. The Palaeozoic history of an unusual intracratonic thrust belt in central Australia based on ^{40}Ar–^{39}Ar, K–Ar and fission track dating. *J. Geol. Soc. Lond.* **149**, 937–954.

Smith, H.A., Giletti, B.J., 1997. Lead diffusion in monazite. *Geochim. Cosmochim. Acta* **61**, 1047–1055.

Spear, F.S., Parrish, R.R., 1996. Petrology and cooling rates of the Valhalla Complex, British Columbia, Canada. *J. Petrol.* **37**, 733–765.

Steiger, R.H., Jäger, E., 1977. Subcommission on geochronology: convention on the use of decay constants in geo- and cosmochronology. *Earth Planet. Sci. Lett.* **36**, 359–362.

Teyssier, C., 1985. A crustal thrust system in an intracratonic environment. *J. Struct. Geol.* **7**, 689–700.

Treloar, P.J., O'Brien, P.J., Parrish, R.R., Khan, M.A., 2003. Exhumation of early Tertiary, coesite-bearing eclogites from the Pakistan Himalaya. *J. Geol. Soc.* **160**, 367–376.

Timmermann, H., Štědrá, V., Gerdes, A., Noble, S.R., Parrish, R.R., Dörr, W., 2004. The problem of dating high-pressure metamorphism: a U–Pb isotope and geochemical study on eclogites and related rocks of the Mariánské Lázně Complex, Czech Republic. *J. Petrol.* **45**, 1311–1338.

Verschure, R.H., Andriessen, P.A.M., Boelrijk, N.A.I.M., Hebeda, E.H., Maijer, C., Priem, H.N.A., Verdurmen, E.A.Th., 1980. On the thermal stability of Rb–Sr and K–Ar biotite systems: Evidence from coexisting Sveconorwegian (ca. 870 Ma) and Caledonian (ca. 400 Ma) biotites in SW Norway. *Contrib. Mineral. Petrol.* **74**, 245–252.

Vry, J.K., Cartwright, I., 1994. Sapphirine–kornerupine rocks from the Reynolds Range, central Australia: constraints on the uplift history of a Proterozoic low pressure terrain. *Contrib. Mineral. Petrol.* **116**, 78–91.

Vry, J.K., Cartwright, I., 1998. Stable isotopic evidence for fluid infiltration during contact metamorphism in a multiply-metamorphosed terrane: the Reynolds Range, Arunta Block, central Australia. *J. Metamorph. Geol.* **16**, 749–765.

Vry, J.K., Compston, W., Cartwright, I., 1996. SHRIMP II dating of zircons and monazites: reassessing the timing of high-grade metamorphism and fluid flow in the Reynolds Range, northern Arunta Block, Australia. *J. Metamorph. Geol.* **14**, 335–350.

Waight, T., Baker, J., Peate, D., 2002a. Sr isotope measurements by double focusing MC-ICPMS: techniques, observations and pitfalls. *Int. J. Mass Spec.* **221**, 229–244.

Waight, T., Baker, J., Willigers, B., 2002b. Rb isotope dilution analyses by MC-ICPMS using Zr to correct for mass fraction-

ation: towards improved Rb–Sr geochronology? *Chem. Geol.* **186**, 99–116.

Williams, I.S., Buick, I.S., Cartwright, I., 1996. An extended episode of early Mesoproterozoic metamorphic fluid flow in the Reynolds Range, central Australia. *J. Metamorph. Geol.* **14**, 29–47.

Willigers, B.J.A., Krogstad, E.J., WiJbrans, J.R., 2001. Comparison of thermochronometers in a slowly cooled granulite terrain: Nagssugtoqidian Orogen, West Greenland. *J. Petrol.* **42**, 1729–1749.

Willigers, B.J.A., Baker, J.A., Krogstad, E.J., Peate, D., 2002. Precise and accurate in situ Pb–Pb dating of apatite, sphene and monazite by laser ablation multiple-collector ICP-MS. *Geochim. Cosmochim. Acta* **66**, 1051–1066.

Willigers, B.J.A., Mezger, K., Baker, J.A., 2004. Development of high precision Rb–Sr phlogopite and biotite geochronology: an alternative to $^{40}Ar/^{39}Ar$ mica dating? *Chem. Geol.* **213**, 339–358.